Large-signal input characteristics of selected DC–DC switching converters, Part II. Discontinuous conduction mode

WŁODZIMIERZ JANKE [ORCID], **MACIEJ BĄCZEK** [ORCID], **JAROSŁAW KRAŚNIEWSKI** [ORCID], **MARCIN WALCZAK** [ORCID]

Department of Electronics and Computer Science
Koszalin University of Technology
Śniadeckich Street 2, 75-453 Koszalin, Poland
e-mails: {wlodzimierz.janke/maciej.baczek/jaroslaw.krasniewski/marcin.walczak}@tu.koszalin.pl

Abstract: Large-signal input characteristics of three DC–DC converter types: buck, boost and flyback working in the discontinuous conduction mode (DCM), obtained by precise large signal PSpice simulations, calculations based on averaged models and measurements are presented. The parasitic resistances of the converter components are included in the simulations. The specific features of the input characteristics in the DCM and the differences between the continuous conduction mode (CCM) and DCM are discussed.

Key words: boost, buck, DC–DC converters, DCM, flyback, input characteristics

1. Introduction

In paper [1], being the first part of this paper series, the importance of the large signal input characteristics of power converters is outlined, essential information concerning the contents of the both parts are given and next the input characteristics of the buck, boost and flyback converters working in the continuous conduction mode (CCM) are discussed. This part is devoted to the input characteristics of the same converters working in the DCM. The input characteristics are investigated by measurements, large signal PSpice simulations and calculations based on averaged models, similarly as in [1]. The explanation of symbols and the description of the components are given in [1]. The schemes of the converters under considerations presented in [1] are shown below (Fig. 1) for convenience.
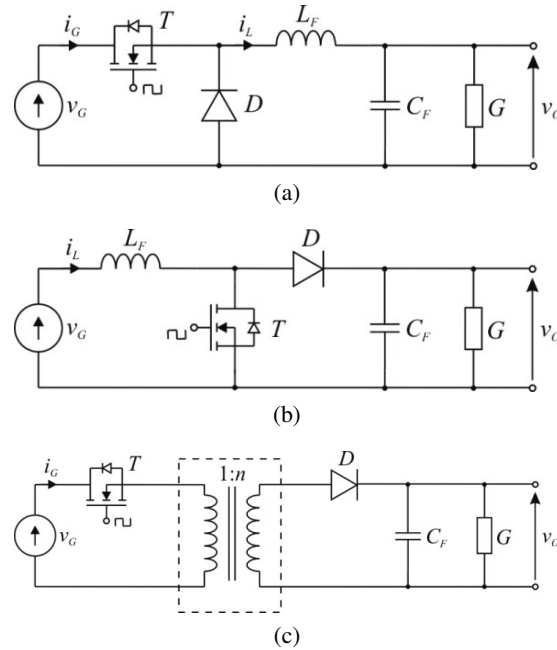
(a)

(b)

(c)

Fig. 1. The power stage of buck (a); boost (b) and flyback (c) converters [1]

In the discontinuous conduction mode, the switching period of a converter containing a single transistor and a single diode consists of three sub-periods: ON (transistor ON, diode OFF), OFF1 (transistor OFF, diode ON) and OFF2 (transistor and diode OFF). The inductor current in the buck and boost, and the current of the magnetizing inductance in the flyback is zero in the sub-period OFF2. A converter works in the DCM, when the load current is sufficiently low. The discontinuous mode of a converter operation may be intentionally obtained or may be a result of the temporary decrease of the converter load current. An approximate condition for DCM steady state operation is that the load conductance value is lower than the critical value G_C, given as:

$$G_C(\text{buck}) = G_Z \cdot (1 - D_A), \tag{1}$$

$$G_C(\text{boost}) = G_Z \cdot D_A \cdot (1 - D_A)^2, \tag{2}$$

$$G_C(\text{flyback}) = \frac{(1 - D_A)^2}{n} \cdot G_Z, \tag{3}$$

where

$$G_Z = \frac{T_S}{2 \cdot L} \tag{4}$$

and L denotes the inductance of a coil or the magnetizing inductance of a transformer.

The important part of this paper (similarly as paper [1]) concerns averaged models of the converters. The averaged model is the approximate description of a converter for time intervals much larger than the switching period. The accuracy of the averaged model depends on the

particulars of its derivation and on the discrepancies between the waveforms of currents assumed in the procedure of averaged model derivation and the real waveforms (as may be observed experimentally). The main advantage of the averaged models is their simplicity. They enable fast simulation of systems composed of several switch-mode converters in the time intervals containing many switching periods. Several approaches to the averaged model derivation are known. The traditional methods presented among others in textbooks cited in [1] are based on so called state-space averaging or on a switch averaging approach. Another approach to creation of the averaged model is based on the separation of variables [2, 3]. The averaged models of ideal simple converters working in the continuous conduction mode (CCM) obtained by the above-mentioned three methods are identical. Models for the DCM obtained by the switch averaging approach differ from the models obtained by two other methods. Models of simple converters (BUCK, BOOST and BUCK-BOOST) obtained by the switch averaging are of the second order (two poles in the small-signal transmittance), whereas the models obtained by state-space averaging or separation of variables are of the first order (single-pole transmittances). This controversy has been mentioned in the literature [4, 5] and there are suggestions (e.g. in [4]) that the models based on the state-space averaging are erroneous. Such opinions have been related to discrepancies between calculations and experiments mentioned, for example, in [4], but have never been precisely proven. It should be pointed out, that the mentioned discrepancies may be the result of errors in measurements as well as the model inaccuracy related, for example, to the process of averaging itself, or the inaccuracy of the description of components.

The waveforms of the input currents in the single switching period obtained by measurements and simulations are presented in Section 2. Section 3 is devoted to averaged models of the buck, boost and flyback in the DCM in the form of equivalent circuits and accompanying equations. The formulas describing the DC input characteristics in the DCM as a special case of the averaged models are given in Section 4. The results of measurements and simulations of the input characteristics in the long time intervals are shown in Section 5.

2. The input current waveforms of the converters in short time intervals

In the laboratory models of buck and boost converters, an NVD5867NLT4G MOS transistor and MBRS340 diode have been used, whereas in a flyback converter the transistor is HEMT TPH3206 and the diode is MBRD1035. The parameters of the converters are: in the buck converter, $L = 90.8$ μH, $C = 108.8$ μF; in the boost converter, $L = 22.6$ μH, $C = 321$ μF; in the flyback converter, L (magnetizing inductance of transformer) is 150 μH and $C = 470$ μF, $n = 0.2$. Switching frequency of the buck is 100 kHz; and of the boost and flyback is 200 kHz. The transistors and diodes in the direct large signal PSpice simulations are represented by their models accessible in the PSpice library. The inductors and capacitors in simulations are treated as a series connections of the ideal elements L and C with parasitic resistances R_L and R_C. The model of the transformer used in the simulation of the flyback converter [1] is shown in Fig. 2. Parasitic parameters of capacitors, inductors and transformer, obtained by the independent measurements and used in Spice simulations (notation in accordance with Figs. 4 and 5 in [1]) are: R_C for the buck, boost and flyback converters are 18.6 mΩ, 70 mΩ and 76 mΩ, respectively,

R_L for the buck and boost converters are 121.6 mΩ and 35 mΩ; R_{L1} is 0.5 Ω, R_{L2} is 23 mΩ. Leakage inductances of the transformer are: L_{R1} = 1.53 μH; L_{R2} = 1.0 nH.
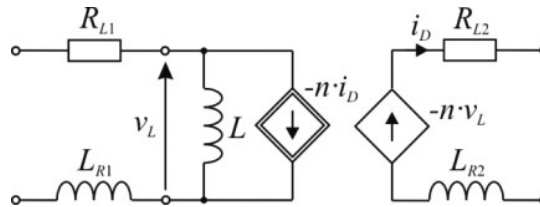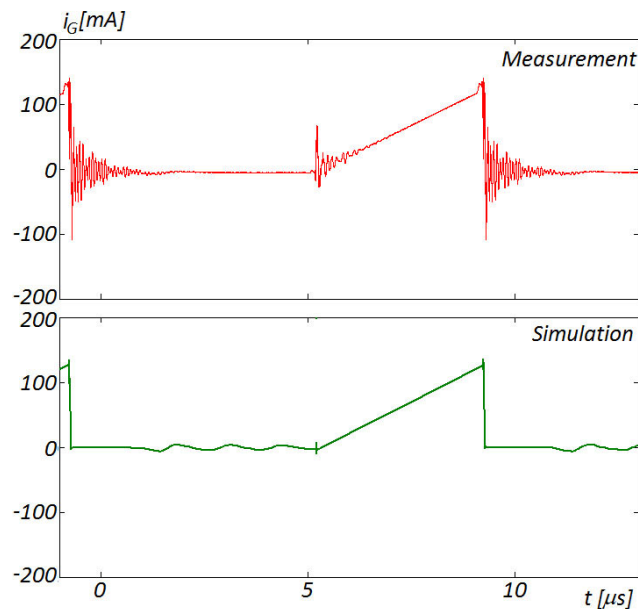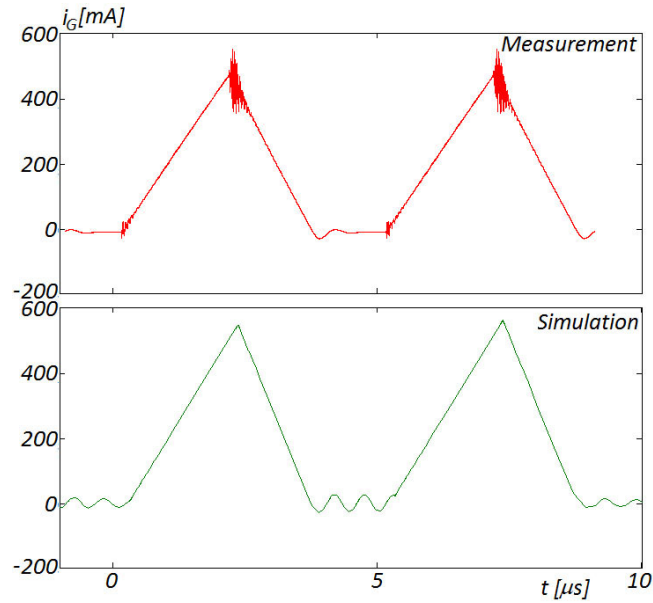

Fig. 2. Model of the transformer used in the large signal PSpice simulations

The examples of the input current waveforms for the power stage of the buck, boost and flyback converters obtained by measurements and large signal PSpice simulations for the short time intervals are shown in Fig. 3. The shape of the waveforms of the input current obtained by measurements and simulations is generally the same, but the differences in the shape of oscillations at the switching instants are visible. The oscillations are caused by parasitic effects in converter components and PCB and these parasitic effects are difficult to describe.

The main, qualitative difference between the input current waveforms in the CCM (see paper [1]) and DCM is the existence of two different forms of the oscillations in the DCM. In the DCM, apart from high frequency oscillations (with the frequency nearly 10 MHz for the flyback converter and higher in the buck and boost converters) at the switching instants, there are slower oscillations (best visible for flyback) of the frequency below 1 MHz, in the time intervals when both switches are OFF.

(a)

(b)
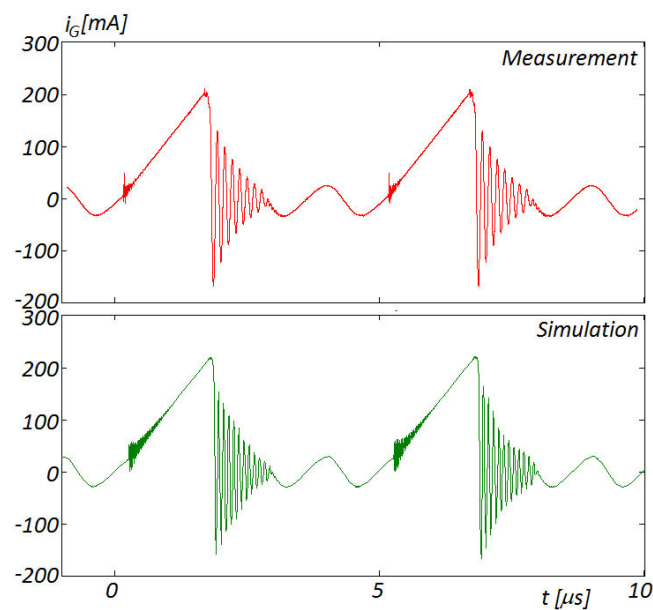
(c)

Fig. 3. Input current waveforms of converters obtained by measurements and large signal PSpice simulations: buck ($v_G = 10$ V, $G = 0.005$ S, $d_A = 0.4$) (a); boost ($v_G = 6$ V, $G = 0.005$ S, $d_A = 0.4$) (b); flyback ($v_G = 20$ V, $G = 0.02$ S, $d_A = 0.3$) (c)

3. Large-signal averaged models of buck, boost and flyback converters for DCM

In the derivation of the large-signal averaged models, the simplified description of components is applied, namely a transistor and diode are described as a series connection of an ideal switch and parasitic resistance R_T or R_D, respectively, whereas the transformer is described in the form of the schematic in Fig. 2 with neglected elements R_{L1}, R_{L2}, L_{R1}, L_{R2}. The resulting averaged models of buck, boost and flyback converters working in the DCM may be presented in the unified form as in Fig. 4, with the different descriptions of the sources i_1 and i_2 [3, 6]. The symbol i_1 corresponds to the input current for all three converter types and the symbol i_2 corresponds to the inductor current in the buck and the diode current in the boost or flyback converters.
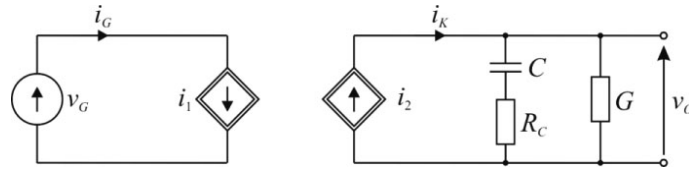

Fig. 4. Large-signal averaged models of buck, boost and flyback converters working in DCM

It is shown in [3] that in the derivation of the averaged models for the DCM, the voltage on the inductor becomes equal to zero, therefore the inductive element is not present in the averaged model. The description of the controlled sources in Fig. 4 for the buck, boost and flyback converters is given below [3, 6]:

$$i_1(\text{buck}) = \frac{(v_G - v_O) \cdot d_A^2}{R_G + R_P \cdot d_A}, \tag{5}$$

$$i_2(\text{buck}) = \frac{(v_G - v_O) \cdot v_G \cdot d_A^2}{v_O \cdot R_G + v_G \cdot R_P \cdot d_A}, \tag{6}$$

$$i_1(\text{boost}) = \frac{G_A \cdot v_G \cdot v_O}{v_O \cdot (1 + d_A \cdot K) - v_G}, \tag{7}$$

$$i_2(\text{boost}) = \frac{G_A \cdot v_G^2}{(v_O \cdot (1 + d_A \cdot K) - v_G) \cdot (1 + d_A \cdot K)}, \tag{8}$$

where:

$$R_G = \frac{1}{G_Z} = \frac{2 \cdot L}{T_S}, \tag{9}$$

$$R_P = R_L + 0.5 \cdot (R_T + R_D), \tag{10}$$

$$K = G_Z \cdot R_P, \tag{11}$$

$$i_1(\text{flyback}) = v_G \cdot G_A \tag{12}$$

and

$$i_2(\text{flyback}) \cong \frac{G_A \cdot v_G^2}{v_O} \cdot \left(1 - \frac{v_G \cdot R_{DL} \cdot d_A \cdot T_S}{v_O \cdot n \cdot L}\right). \tag{13}$$

It should be pointed out that the current i_1 of the buck and boost converter models depends on both voltages v_G and v_O whereas in the flyback converter model it depends only on the input voltage v_G. As a consequence Eq. (9), describing the current i_2, is not necessary in calculations of the input characteristics of the flyback converter working in the DCM.

4. DC input characteristics

In the averaged models, the DC input characteristics of converters working in the discontinuous conduction mode are obtained from the equivalent circuit presented in Fig. 4 and Eqs. (5)–(13). The dependencies of the DC input current I_{IN} on the input voltage V_G for the non-ideal buck and boost converters in the DCM (with the series resistances included) are described by Eqs. (14) and (15).

A) Buck

$$I_G = \frac{V_G \cdot D_A^2 \cdot \left[2 \cdot R_G + D_A \cdot \left[R_P + D_A \cdot R - \sqrt{4 \cdot R \cdot R_G + (R_P + D_A \cdot R)^2}\right]\right]}{2 \cdot R_G \cdot (R_G + D_A \cdot R_P)}, \quad (14)$$

B) Boost

$$I_G = -\frac{G_A \cdot V_G \cdot \left[1 + \sqrt{(4 \cdot G_A \cdot R + 1) \cdot (D_A \cdot K + 1)^2} + D_A \cdot K\right]}{(D_A \cdot K + 1) \cdot \left[1 - \sqrt{(4 \cdot G_A \cdot R + 1) \cdot (D_A \cdot K + 1)^2} + D_A \cdot K\right]}, \quad (15)$$

C) Flyback.

The DC input characteristics for non-ideal flyback may be presented also in the analytical form but it is very involved, therefore the simplified form is given below for the ideal converter (without parasitic resistances). The input conductance of the flyback converter working in the DCM, according to paper [6] is equal to G_A given by Eq. (16):

$$G_A = D_A^2 \cdot G_Z. \quad (16)$$

Therefore:

$$I_G \cong G_A \cdot V_G. \quad (17)$$

5. Calculations and measurements of the input characteristics for DC or the large time intervals

The input characteristics of converters working in the discontinuous conduction mode for large time intervals $\Delta t \gg T_S$, obtained by large signal PSpice simulations, calculations based on averaged models and measurements are presented below. The structure of the set of measurements and simulations is similar to that in paper [1], but the operation of the converters in DCM corresponds to lower values of the load conductance in the CCM.

5.1. DC input characteristics

The examples of the dependencies of the DC term of the input current on the input voltage, obtained by measurements and simulations are shown in Figs. 5(a), (b) and (c). Two kinds of
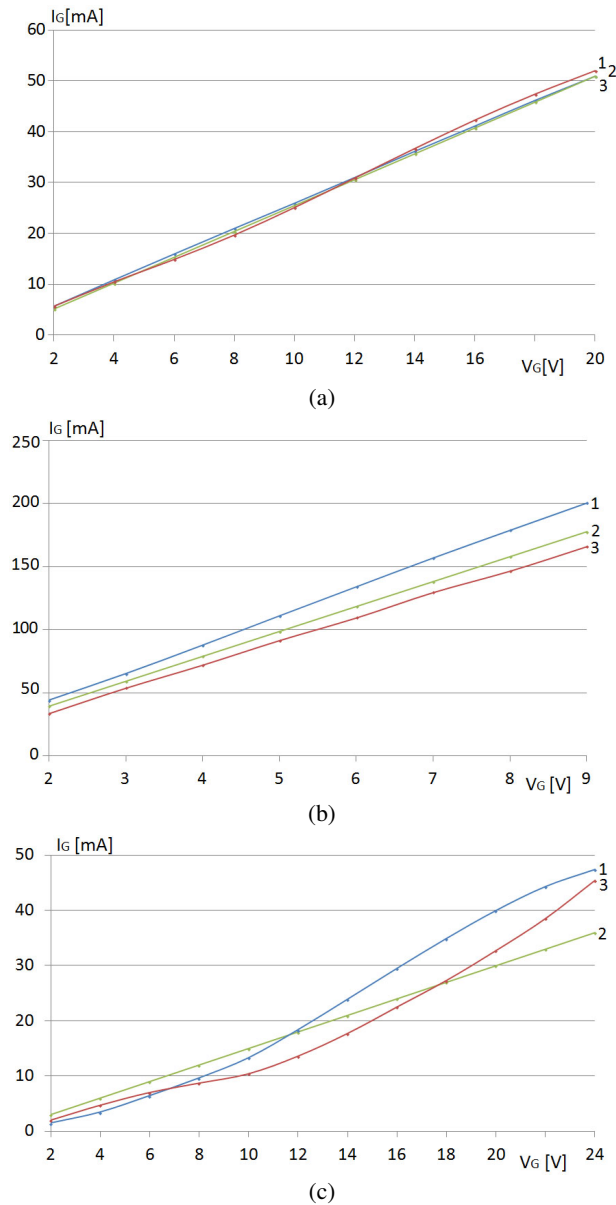

Fig. 5. Dependence of the DC input current I_G on the input voltage V_G for converters: buck (a); boost (b) and flyback (c). Curves: 1 – large signal PSpice simulations; 2 – calculations on Eqs. (14)–(17); 3 – measurements. Duty ratio for all converters is $D_A = 0.3$, load resistance for buck and boost is 200 Ω and for flyback is 50 Ω

simulations are presented – based on analytical Formulas (14), (15) and (17), resulting from the averaged models, and based on large signal PSpice simulations for a steady state. The deviation from the linearity, caused by parasitic resistances is best visible in the case of the flyback converter.
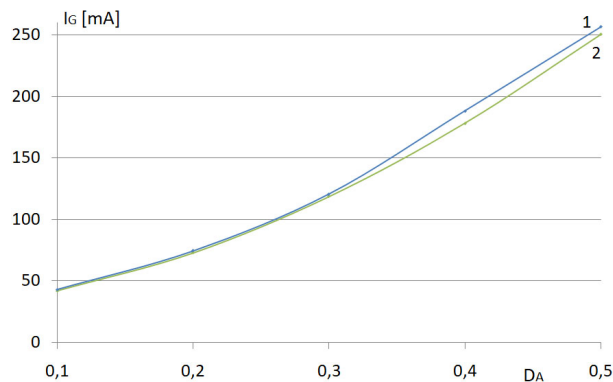

Fig. 6. Dependence of I_G on D_A for boost converter with input voltage $V_G = 6$ V, load resistance
$R = 200$ Ω, curve 1 – large signal PSpice simulations, 2 – calculations on Eqs. (15)–(17)

According to Eqs. (14)–(17), the DC term of the input current (in the averaged models) is proportional to the square of the duty ratio. The exemplary dependence of I_G on D_A, obtained by large signal PSpice simulations and averaged model simulation for the boost converter (Fig. 9), confirms this dependence.

5.2. Time-domain input characteristics

The examples of the time-domain input characteristics of converters, in the form of the input current response to the step change of the input voltage or duty ratio, for time intervals containing many switching periods are shown in Figs. 7, 8 and 9 for the buck, boost and flyback converters, respectively. In the figure captions, the step change of a given quantity is described in the exemplary form – v_G: 8–10 V, whereas the constant quantity is marked in the figure. Curves 1 in Figs. 7–9 denote results of the detailed, large signal PSpice simulations, curves 2 – simulations based on the averaged models and 3 – measurements.

The results of measurements, large signal PSpice simulations and simulations based on the averaged models are consistent for buck and boost converters, as it is seen in Figs. 7 and 8. In the case of the flyback converter, the calculations based on the averaged model differ from other results. The procedure of the averaged model creation itself is seriously simplified and in the case of the flyback converter, the additional inaccuracy is probably introduced by the use of the oversimplified model of the transformer in the derivation of the averaged model. The specific behavior of the flyback converter visible in Fig. 6 may be related to the fact, that, according to the averaged model, the current i_1, described by Eq. (8) in the model, is independent of the output voltage.

The shapes of the input current waveforms corresponding to the step change of the input voltage or duty ratio, obtained for the converters working in the DCM differ substantially from
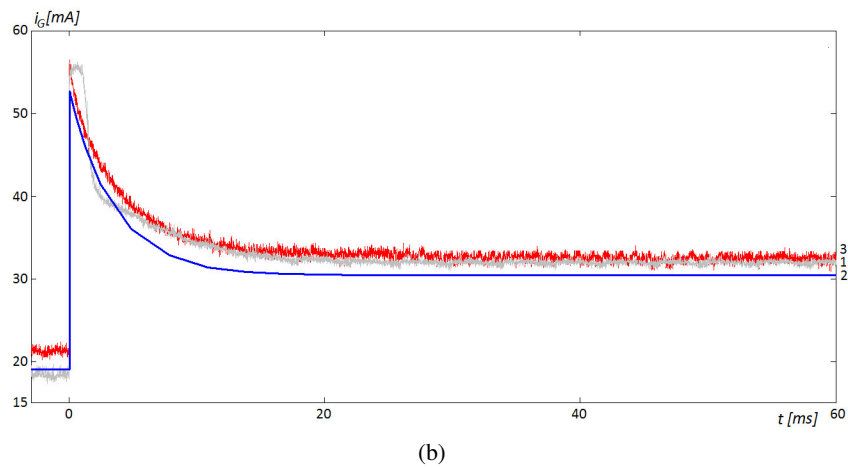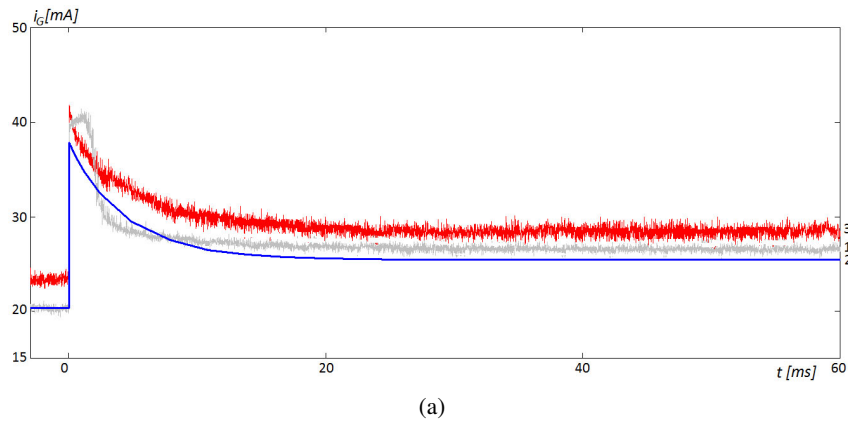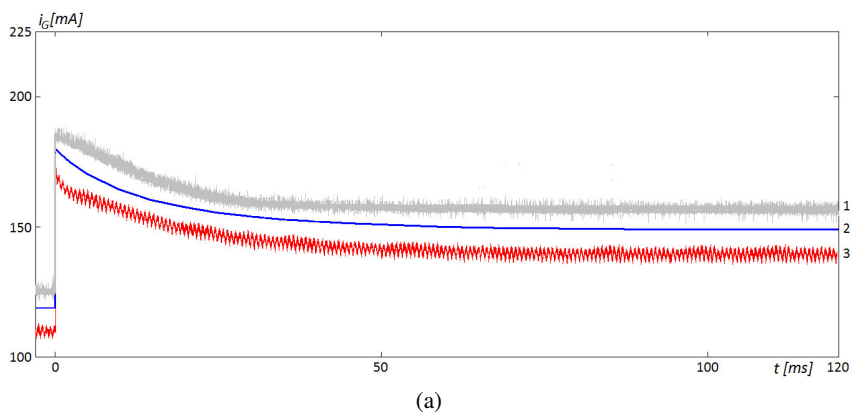
(a)

(b)

Fig. 7. The input current response i_G in buck converter: to the input voltage step from 8 to 10 V
for $D_A = 0.4$ (a); to the duty ratio step from 0.3 to 0.5 for $V_G = 10$ V (b); ($R = 200$ Ω)
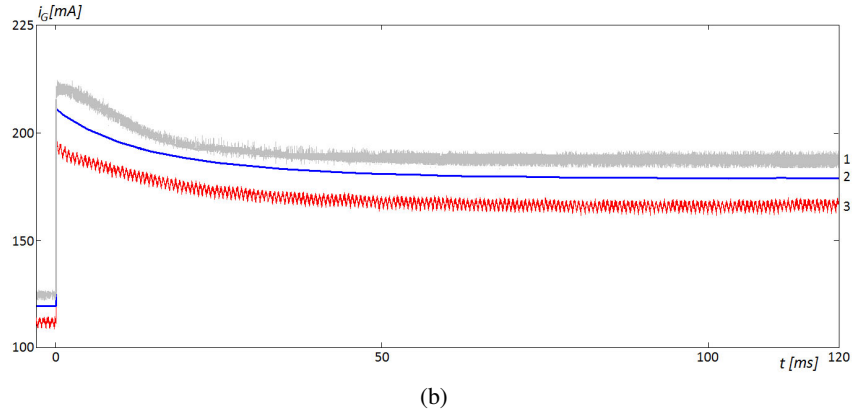

(a)

(b)

Fig. 8. The input current response i_G in boost converter: to the input voltage step from 4 to 5 V for $D_A = 0.4$ (a); to the duty ratio step from 0.3 to 0.4 for $V_G = 6$ V (b); ($R = 200\ \Omega$)
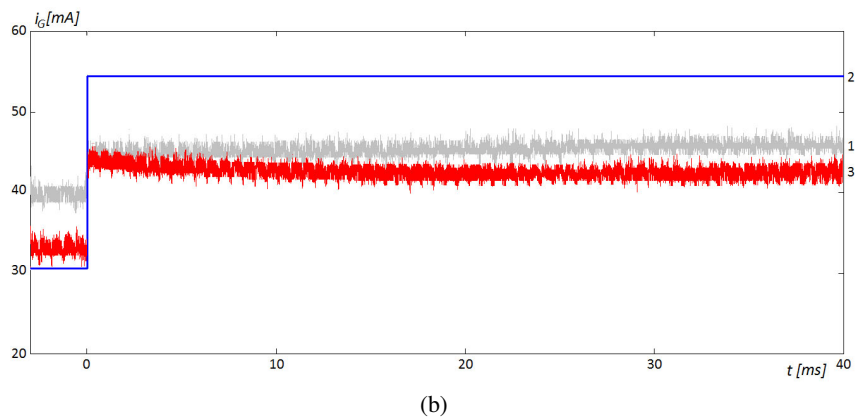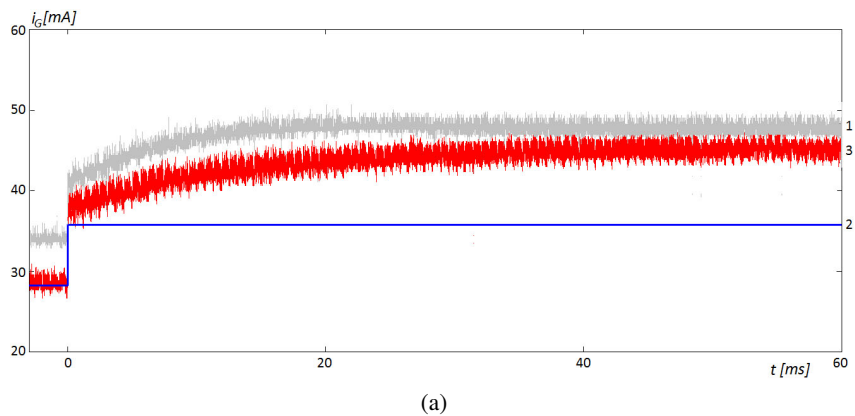

(a)

(b)

Fig. 9. The input current response i_G in flyback converter: to the input voltage step from 18 to 24 V for $D_A = 0.3$ (a); to the duty ratio step from 0.3 to 0.4 for $V_G = 20$ V (b); ($R = 200\ \Omega$)

those obtained for the CCM, presented in [1]. The responses for the converters in the CCM are oscillating, that is typical to a second-order transmittance. The responses for the buck and boost converters working in the DCM corresponds approximately to the first-order transmittance. It may be observed, that the time constants corresponding to the input current waveforms obtained as the response to the step change of the input voltage or duty ratio for the buck and boost converters differ from time constants calculated as the product $R \cdot C$ of the output capacitance and the load resistance, and from the time constants of the output voltage response. It may be explained as the result of the specific features of the converters working in the DCM, that is represented by the scheme shown in Fig. 4 and Eqs. (5)–(8), in which the nonlinear controlled sources are present that is equivalent to the existence of the nonlinear feedback.

The exemplary time constants describing the input current waveforms of the buck and boost converters are given in Table 1. The first letter in the column "conditions" denotes: A – buck, B – boost. The second letter denotes: A – response to the input voltage step, B – response to the duty ratio step.

Table 1. Approximate values of time constants (in milliseconds) corresponding to the shape of the input current waveforms obtained after step change of the input voltage or duty ratio

Conditions	Measurements	Large signal PSpice simulations	Averaged model	$R \cdot C$
AA	4.5	2.3	4.5	21.5
AB	3.6	2	3.5	
BA	16.5	16.5	15.5	63.5
BB	15	12.5	15	

6. Summary and conclusions

The large-signal input characteristics of the power stage of DC–DC converters: buck, boost and flyback, working in the discontinuous conduction mode (DCM), are presented. The characteristics are obtained by measurements, large signal PSpice simulations and simulations based on averaged models. The parasitic resistances of the converters components are taken into account in simulations.

In Section 2 – the fast changes of the input current in the time intervals comparable with the switching period are shown. Parasitic oscillations visible at switching instances are different in nature for particular converters. The averaged models of the converters are discussed in Section 3 describing the converter's behavior in the large time intervals. Measurements and simulations for large time intervals are presented in Sections 4 and 5.

The main observations concerning the input characteristics of the converters in the DCM are as follows:

1. The waveforms of the input current inside the single switching interval (Section 2) in CCM and DCM are similar apart from the existence of the OFF2 subinterval in the DCM, in

which the oscillations observed are of lower frequency than the oscillations immediately after switching-off the transistor.

2. The DC dependence of the input current on the input voltage are nearly linear, similarly as in the CCM, but the slopes in the CCM and DCM are different. This is caused mainly by the difference in load resistance.

3. The dynamic input characteristics of the converters in the DCM have the features of the first order systems and differ from that in the CCM corresponding to the second order system.

4. The time constants corresponding to the input current response to the step change of the input voltage or duty ratio for buck and boost converters in the DCM differ from the product $R \cdot C$ of the load resistance and the output capacitance (see Table 1).

5. The simulation results of the input characteristics of the converters in the DCM performed with the use of averaged models are, in general, consistent with the measurements and large signal PSpice simulations, with the exception of the dynamic behavior of the flyback converter. The inaccuracy of the flyback description based on the averaged model may be caused by the use of the oversimplified model of a transformer in the averaged model derivation for a flyback converter.

References

Only the references mentioned in the above text are listed below.
The full list of references is in paper [1].

[1] Janke W., Bączek M., Kraśniewski J., Walczak M., *Large-signal input characteristics of selected DC–DC switching converters. Part I. Continuous conduction mode*, submitted to Archives of Electrical Engineering, vol. 69, no. 3, pp. 738–750 (2020).

[2] Janke W., *Averaged Models of Pulse-Modulated DC–DC Converters, Part II. Models Based on the Separation of Variables*, Archives of Electrical Engineering, vol. 61, no. 4, pp. 633–654 (2012).

[3] Janke W., *Equivalent circuits for averaged description of DC–DC switch-mode power converters based on separation of variables approach*, Bulletin of the Polish Academy of Sciences, vol. 61, no. 3 (2013).

[4] Sun J., Mitchell D., Greuel M., Krein P., Bass R., *Averaged modeling of PWM Converters Operating in Discontinuous Conduction Mode*, IEEE Transactions on Power Electronics, vol. 16, no. 4, pp. 482–492 (2001).

[5] Vu T.T., *Non-linear Dynamic Transformer Modelling and Optimum Control Design of Switched-mode Power Supplies*, PhD Thesis, National University of Ireland, Maynooth (2014).

[6] Janke W., Bączek M., Kraśniewski J., *Input characteristics of a non-ideal DC–DC flyback converter*, Bulletin of the Polish Academy of Sciences: Technical Sciences, vol. 67, no. 5, pp. 841–849 (2019).